

Intermediate triplet states in the reverse inter-system crossing of MR-TADF emitters

Herbert D. Ludowieg

Department of Chemistry, University at Buffalo, State University of New York

October 19, 2021

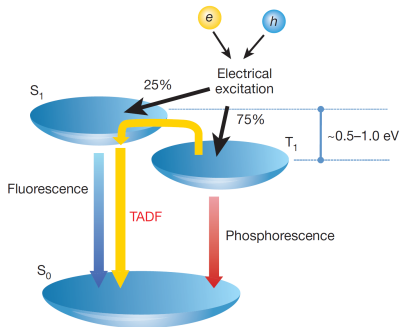
- OLEDs were first observed in 1987 and are now a widely used technology for electronic displays
- New smartphones like the Samsung Galaxy Z Flip uses an OLED screen

- OLEDs were first observed in 1987 and are now a widely used technology for electronic displays
- New smartphones like the Samsung Galaxy Z Flip uses an OLED screen
- LCD displays are the most widely used type of display technology
- LCD displays suffer from less than ideal contrast where OLED has proven to have great color contrast

Introduction

$$\eta_{\text{ext}} = \eta_{\text{int}}\eta_{\text{out}} \quad \eta_{\text{out}} \approx \frac{1}{2n^2}$$

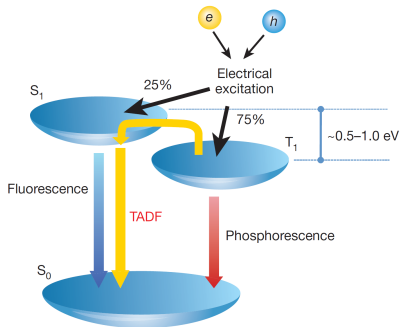
- Under electrical excitation exciton formation is in a 1:3 ratio to singlet and triplet excited states
- First generation OLEDs relied on fluorescence



Introduction

$$\eta_{\text{ext}} = \eta_{\text{int}}\eta_{\text{out}} \quad \eta_{\text{out}} \approx \frac{1}{2n^2}$$

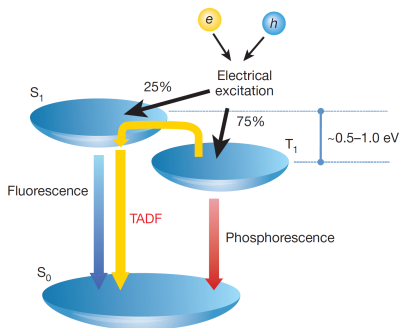
- Under electrical excitation exciton formation is in a 1:3 ratio to singlet and triplet excited states
- First generation OLEDs relied on fluorescence
 - Can rely on organic compounds



Introduction

$$\eta_{\text{ext}} = \eta_{\text{int}}\eta_{\text{out}} \quad \eta_{\text{out}} \approx \frac{1}{2n^2}$$

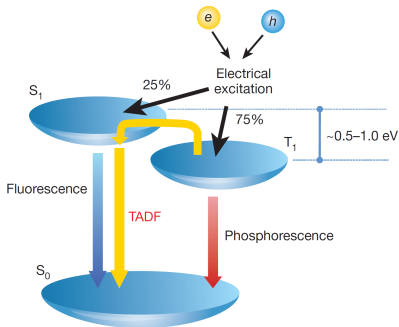
- Under electrical excitation exciton formation is in a 1:3 ratio to singlet and triplet excited states
- First generation OLEDs relied on fluorescence
 - Can rely on organic compounds
 - Maximum theoretical internal quantum efficiency locked to 25%



Introduction

$$\eta_{\text{ext}} = \eta_{\text{int}}\eta_{\text{out}} \quad \eta_{\text{out}} \approx \frac{1}{2n^2}$$

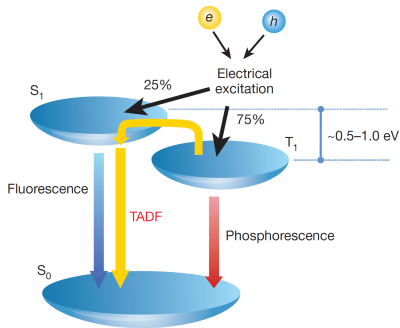
- Under electrical excitation exciton formation is in a 1:3 ratio to singlet and triplet excited states
- Second generation OLEDs relied on phosphorescence



Introduction

$$\eta_{\text{ext}} = \eta_{\text{int}}\eta_{\text{out}} \quad \eta_{\text{out}} \approx \frac{1}{2n^2}$$

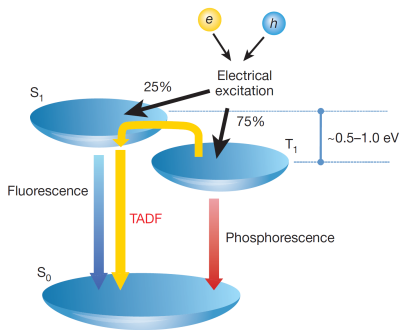
- Under electrical excitation exciton formation is in a 1:3 ratio to singlet and triplet excited states
- Second generation OLEDs relied on phosphorescence
 - Maximum theoretical internal quantum efficiency locked to 75%



Introduction

$$\eta_{\text{ext}} = \eta_{\text{int}}\eta_{\text{out}} \quad \eta_{\text{out}} \approx \frac{1}{2n^2}$$

- Under electrical excitation exciton formation is in a 1:3 ratio to singlet and triplet excited states
- Second generation OLEDs relied on phosphorescence
 - Maximum theoretical internal quantum efficiency locked to 75%
 - Require spin-orbit effects coming from cyclometalated complexes
 - Metals include Ir, Pt, Pd, Eu, and Tb



Thermally activated delayed fluorescence (TADF)

- Pioneered by Parker and Hatchard¹ who noticed delayed fluorescence from eosin in solution

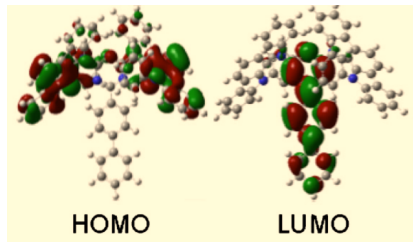
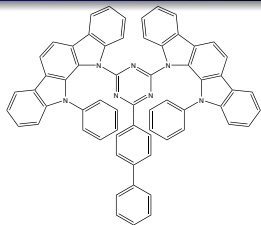


Figure: Reproduced from Ref. 2

¹Parker, and Hatchard *Trans. Faraday Soc.*, **1961**, *57*, 1894–1904

²Endo, et al *Appl. Phys. Lett.*, **2011**, *98*, 083302

³Uoyama, et al *Nature*, **2012**, *492*, 234–238

Thermally activated delayed fluorescence (TADF)

- Pioneered by Parker and Hatchard¹ who noticed delayed fluorescence from eosin in solution
- Later work by Endo et al.² showed the first TADF emitter which involved spatial separation of donor and acceptor (D-A) moieties

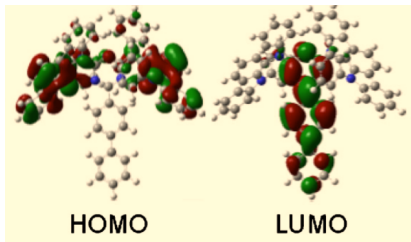
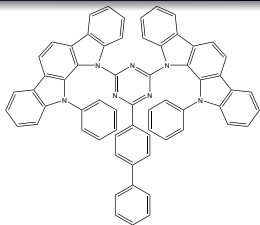


Figure: Reproduced from Ref. 2

¹Parker, and Hatchard *Trans. Faraday Soc.*, **1961**, *57*, 1894–1904

²Endo, et al *Appl. Phys. Lett.*, **2011**, *98*, 083302

³Uoyama, et al *Nature*, **2012**, *492*, 234–238

Thermally activated delayed fluorescence (TADF)

- Pioneered by Parker and Hatchard¹ who noticed delayed fluorescence from eosin in solution
- Later work by Endo et al.² showed the first TADF emitter which involved spatial separation of donor and acceptor (D-A) moieties
- Uoyama et al.³ were then able to create a series of TADF emitters that were more efficient than conventional OLEDs

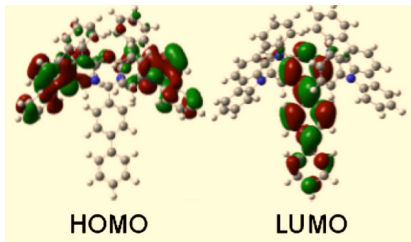
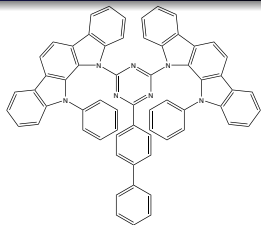


Figure: Reproduced from Ref. 2

¹Parker, and Hatchard *Trans. Faraday Soc.*, **1961**, 57, 1894–1904

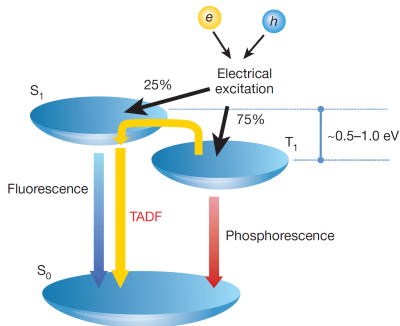
²Endo, et al *Appl. Phys. Lett.*, **2011**, 98, 083302

³Uoyama, et al *Nature*, **2012**, 492, 234–238

Thermally activated delayed fluorescence (TADF)

$$\eta_{\text{ext}} = \eta_{\text{int}}\eta_{\text{out}} \quad \eta_{\text{out}} \approx \frac{1}{2n^2}$$

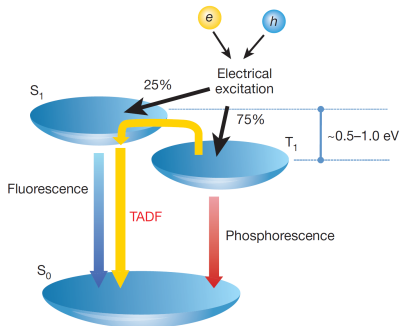
- The driving force is reverse intersystem crossing (rISC)
- Excitons in the triplet state can upconvert into the singlet state



Thermally activated delayed fluorescence (TADF)

$$\eta_{\text{ext}} = \eta_{\text{int}}\eta_{\text{out}} \quad \eta_{\text{out}} \approx \frac{1}{2n^2}$$

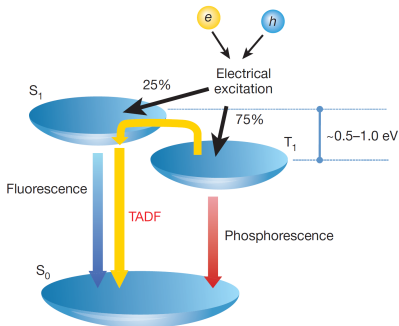
- The driving force is reverse intersystem crossing (rISC)
- Excitons in the triplet state can upconvert into the singlet state
- This then increased the maximum theoretical internal quantum efficiency to 100%



Thermally activated delayed fluorescence (TADF)

$$\eta_{\text{ext}} = \eta_{\text{int}}\eta_{\text{out}} \quad \eta_{\text{out}} \approx \frac{1}{2n^2}$$

- The driving force is reverse intersystem crossing (rISC)
- Excitons in the triplet state can upconvert into the singlet state
- This then increased the maximum theoretical internal quantum efficiency to 100%
- Can also use fully organic molecules as we only rely on fluorescence



- Generally $E_{S_1} - E_{T_1} < 0.20$ eV ($\Delta E_{S_1T_1}$)
- D-A TADF emitters have allowed researchers better control over $\Delta E_{S_1T_1}$

- Generally $E_{S_1} - E_{T_1} < 0.20$ eV ($\Delta E_{S_1T_1}$)
- D-A TADF emitters have allowed researchers better control over $\Delta E_{S_1T_1}$
- Can generate a broad range of colors thanks to the control over the HOMO–LUMO gap

- Generally $E_{S_1} - E_{T_1} < 0.20$ eV ($\Delta E_{S_1T_1}$)
- D-A TADF emitters have allowed researchers better control over $\Delta E_{S_1T_1}$
- Can generate a broad range of colors thanks to the control over the HOMO–LUMO gap
- Have also allowed significant structural relaxation which has led to broad emission bandwidths
- Achieving high photoluminescence quantum yields (PLQY) and color purity has proven challenging

Multi-resonance TADF (MR-TADF)

- In 2016 Hatakeyama et al. were able to make a notable departure from the usual strategy
- They designed a pair of TADF emitters with a triangulene core with *ortho*-substituted boron and nitrogen atoms
- This thereby promoted resonance effects

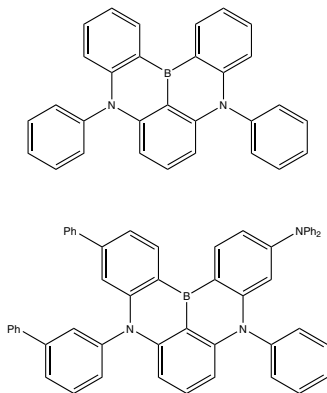


Figure: Top: **DABNA-1** Bottom: **DABNA-2**

Multi-resonance TADF (MR-TADF)

- In 2016 Hatakeyama et al. were able to make a notable departure from the usual strategy
- They designed a pair of TADF emitters with a triangulene core with *ortho*-substituted boron and nitrogen atoms
- This thereby promoted resonance effects
- Were able to generate very narrow emission spectra with high EQE for a pure blue emission

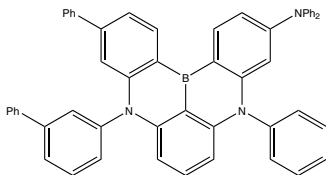
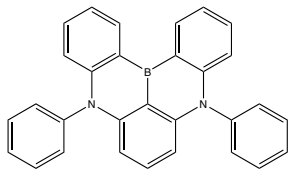


Figure: Top: **DABNA-1** Bottom: **DABNA-2**

- These new class of molecules opened the door to be a potential candidate
- Now need emitters in the green and red regions for modern displays
- Recently, a MR-TADF emitter has been reported by Yang, Park, and Yasuda that could emit at 615 nm (red)
- There is much promise as we can achieve emission bandwidths of 18 nm and EQE of 34.4%

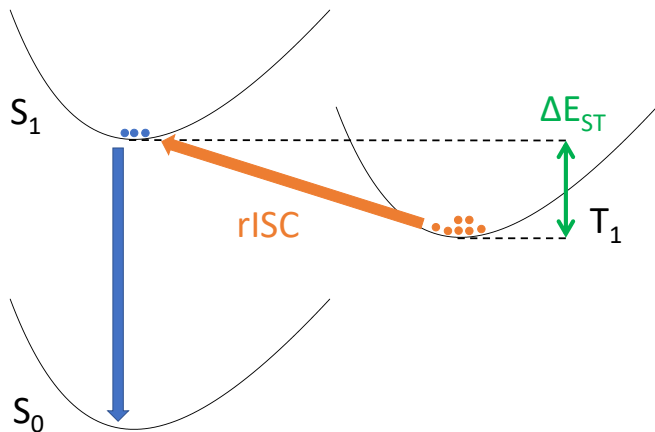
- Previous studies for D-A TADF emitters have used popular DFT functionals
- Due to the charge-transfer states involved, calculations employing the Tamm-Dancoff Approximation (TDA) have to be used

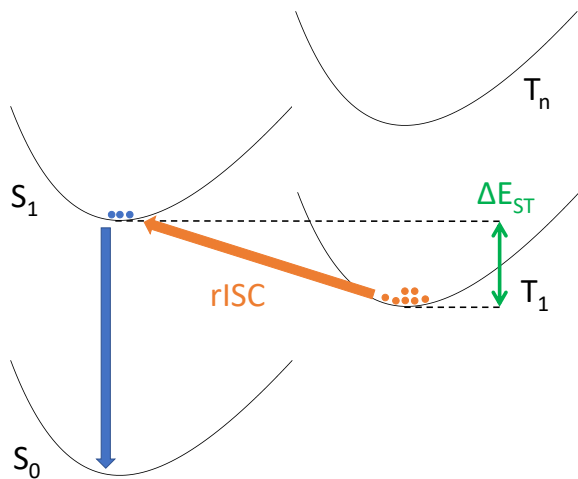
- Previous studies for D-A TADF emitters have used popular DFT functionals
- Due to the charge-transfer states involved, calculations employing the Tamm-Dancoff Approximation (TDA) have to be used
- Previous studies by Pershin et al. showed that popular DFT functionals failed to reproduce $\Delta E_{S_1T_1}$ for MR-TADF

- Previous studies for D-A TADF emitters have used popular DFT functionals
- Due to the charge-transfer states involved, calculations employing the Tamm-Dancoff Approximation (TDA) have to be used
- Previous studies by Pershin et al. showed that popular DFT functionals failed to reproduce $\Delta E_{S_1T_1}$ for MR-TADF
- Only when higher-level Spin-Component Scaling second-order approximate Coupled Cluster (SCS-CC2) theory were used was $\Delta E_{S_1T_1}$ reproduced well to experiment

Table: $\Delta E_{S_1T_1}$ data for **DABNA-1** by Pershin et al

Method	Type	$\Delta E_{S_1T_1}$
VWN	LDA	0.25
PBE	GGA	0.34
PBE0	HYB (25 % HF ex)	0.53
BH-LYP	HYB (50 % HF ex)	0.76
ω B97	$\omega=0.17$	0.52
HF	CIS	1.14
CC2	cc-pVDZ	0.19
	def2-TZVP	0.17
SCS-CC2	cc-pVDZ	0.17
	def2-TZVP	0.15
STEOM-CCSD	cc-pVDZ	0.12
Experimental		0.15



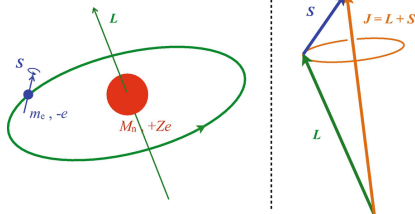


Triplet states involved in rISC

- Over the past few years there have been a number of theoretical studies which have tried to study the complex behavior of the rISC in **DABNA-1**
- There is some general agreement that k_{rISC} is facilitated by nearby triplet states
- However, there is some disagreement on which state is involved
- May be due to the complex nature of the way the states couple with each other via direct spin-orbit coupling and spin-vibronic coupling

Spin-orbit coupling (SOC)

- Relativistic effect that acts on both angular momentum and spin, allowing states of different multiplicity to couple
- Important when considering ISC and phosphorescence as in second generation OLEDs



Nonadiabatic coupling (Vibronic coupling)

- Coupling of electronic states with vibrational degrees of freedom
- Breaks the Born-Oppenheimer approximation as we now couple the nuclear and electronic degrees of freedom

Nonadiabatic coupling (Vibronic coupling)

- Coupling of electronic states with vibrational degrees of freedom
- Breaks the Born-Oppenheimer approximation as we now couple the nuclear and electronic degrees of freedom
- Often described by the Herzberg-Teller approximation

$$\begin{aligned}\mathbf{\Lambda}_{1,2} &= \sum_p^M \langle \phi_1 | Q_p | \phi_2 \rangle \left. \frac{\partial \mathbf{\Lambda}_{1,2}^e(Q)}{\partial Q_p} \right|_0 \\ \frac{\partial \mathbf{\Lambda}_{1,2}^e(Q)}{\partial Q_p} &= \sum_{k \neq 1} \langle \psi_k^0 | \mathbf{\Lambda}_{1,2}^e | \psi_2^0 \rangle \frac{\partial \langle \psi_1^0 | H | \psi_k^0 \rangle / \partial Q_p}{E_1^0 - E_k^0} \\ &\quad + \sum_{k \neq 2} \langle \psi_1^0 | \mathbf{\Lambda}_{1,2}^e | \psi_k^0 \rangle \frac{\partial \langle \psi_k^0 | H | \psi_2^0 \rangle / \partial Q_p}{E_2^0 - E_k^0}\end{aligned}$$

Spin-vibronic coupling (SVC)

- SOC is typically limited to a specific nuclear configuration
- Sometimes the effects of nuclear motions on SOC must be taken into account

Spin-vibronic coupling (SVC)

- SOC is typically limited to a specific nuclear configuration
- Sometimes the effects of nuclear motions on SOC must be taken into account
- SVC occurs when states are mixed by vibronic and SO coupling simultaneously
- Complex behavior that must be taken into account by quantum dynamics simulations

Spin-vibronic coupling (SVC)

- SOC is typically limited to a specific nuclear configuration
- Sometimes the effects of nuclear motions on SOC must be taken into account
- SVC occurs when states are mixed by vibronic and SO coupling simultaneously
- Complex behavior that must be taken into account by quantum dynamics simulations
- One type of QD simulation which has been employed is the multi-configuration time-dependent Hartree (MCTDH)

Spin-vibronic coupling (SVC)

- SOC is typically limited to a specific nuclear configuration
- Sometimes the effects of nuclear motions on SOC must be taken into account
- SVC occurs when states are mixed by vibronic and SO coupling simultaneously
- Complex behavior that must be taken into account by quantum dynamics simulations
- One type of QD simulation which has been employed is the multi-configuration time-dependent Hartree (MCTDH)
- Recent study by Kim et al highlighted on how the SVC dominated k_{rISC}

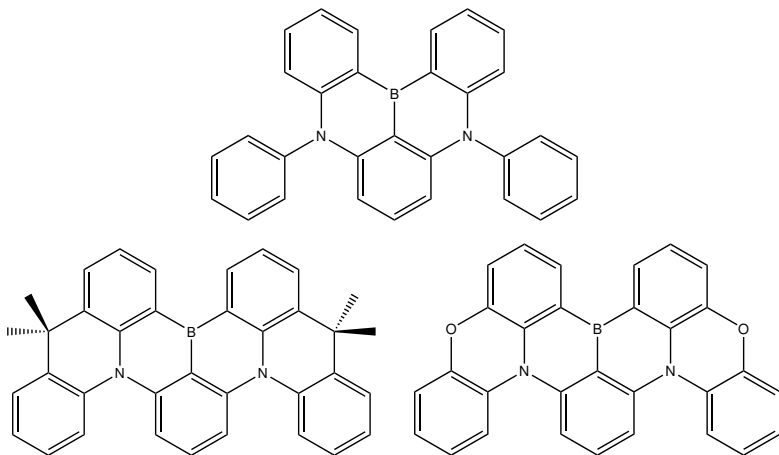


Figure: Top: **DABNA-1**¹. Left: **DMAc-BN**². Right: **PXZ-BN**².

¹Hatakeyama, et al *Adv. Mater.* **2016**, *28*, 2777–2781

²Liu, et al *J. Mater. chem. C* **2021**, *9*, 8308–8313

Table: λ_{em} are the emission wavelengths. Φ_{PL} is the photoluminescence yields. τ_{PF} , and τ_{DF} are the prompt and delayed fluorescence decay lifetimes, respectively.

Emitter	λ_{em} (nm)	FWHM (nm)	$\Delta E_{\text{S}_1\text{T}_1}$ (eV)	Φ_{PL} (%)	τ_{PF} (ns)	τ_{DF} (μs)	EQE (%)
DABNA-1 ¹	460	30	0.20	88	8.8	93.7	13.5
DMAc-BN ²	484	33	0.16	88	6.2	32.9	20.3
PXZ-BN ²	502	38	0.17	90	8.2	90.7	23.3

¹Hatakeyama, et al *Adv. Mater.* **2016**, *28*, 2777–2781

²Liu, et al *J. Mater. chem. C* **2021**, *9*, 8308–8313

Proposed research

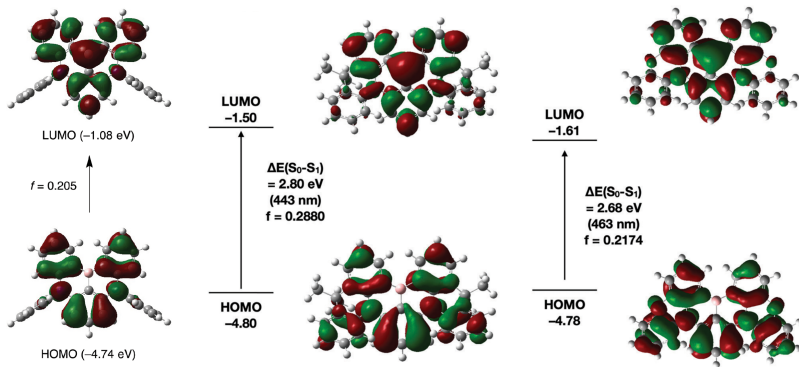


Figure: HOMO and LUMO isosurface plots of **DABNA-1¹** (left), **DMAc-BN²** (center), **PXZ-BN²** (right).

¹Hatakeyama, et al *Adv. Mater.* **2016**, *28*, 2777–2781

²Liu, et al *J. Mater. chem. C* **2021**, *9*, 8308–8313

- Perform a study on **DABNA-1**, **DMAc-BN**, **PXZ-BN**
- Attempt to find similarities in the electronic structure of the molecules along with the vibrational modes which contribute most to the SVC
- This can give us more information that can lead to better materials being discovered
- Already see that the LUMO of the molecules are very similar
- If there is a systematic relation between the vibrational modes it is also possible to perform better studies where we can neglect certain vibrational modes by symmetry

- Will concentrate on the role of O against $C(CH_3)_2$
- Comparisons between **DMAc-BN** and **PXZ-BN** may highlight a greater understanding on the role of electron withdrawing groups in stabilizing/destabilizing nearby triplet states
- The destabilization of the triplet states is believed to be the reason for the increased τ_{DF} in **DMAc-BN** against **PXZ-BN**

- For all electronic structure calculations we will use the highly accurate CASSCF/CASPT2 methods as implemented in the Molcas/OpenMolcas program package
- Spin-orbit effects will be considered via RASSI among the spin-free states
- Potential energy surfaces will be calculated following the derivation on Ref. 1 and 2
- Geometry optimizations and harmonic frequency calculations will be performed with the Gaussian program package
- Quantum dynamics simulations will be performed with the multi-configuration time-dependent Hartree method

¹Jouybari, Liu, Improta, Santoro *J. Chem. Theory Comput.*, **2020**, *16*, 5792–5808

²Aleotti et al. *J. Chem. Phys.*, **2021**, *154*, 104106

- Perform a full CI expansion on the chosen AS
- Direct control over which states are in the wavefunction
- Can perform a more in-depth study to the role of each state and how they couple with each other
- Can build PES for the quantum dynamics simulations based on the chosen wavefunction
- When a suitable AS is chosen we can generate very accurate and reliable data

$$\mathbf{H}^{\text{SO-vib}} = \mathbf{H}^{\text{SO}} + \mathbf{H}^{\text{vib}}$$

$$\mathbf{H}^{\text{vib}} = \mathbf{H}^{(0)} + \mathbf{W}^{(0)} + \mathbf{W}^{(1)} + \mathbf{W}^{(2)} + \dots$$

- The zeroth order Hamiltonian, $\mathbf{H}^{(0)}$, can be expressed using a ground state harmonic oscillator approximation

$$\mathbf{H}^{(0)} = \sum_{\alpha} \frac{\omega_{\alpha}}{2} \left(\frac{\partial^2}{\partial Q_{\alpha}^2} + Q_{\alpha}^2 \right)$$

- The zeroth order expansion term, $\mathbf{W}^{(0)}$, is typically represented by the adiabatic energies as the adiabatic and diabatic potential energy surfaces (PES) are equal

$$\mathbf{H}^{\text{vib}} = \mathbf{H}^{(0)} + \mathbf{W}^{(0)} + \mathbf{W}^{(1)} + \mathbf{W}^{(2)} + \dots$$

- The first order expansion term, $\mathbf{W}^{(1)}$, is the linear vibronic coupling (LVC) model given by

$$\mathbf{W}_{ij}^{(1)} = \sum_{\alpha} \langle \Phi_i(Q_0) | \partial \mathbf{H}_{\text{el}} / \partial Q_{\alpha} | \Phi_j(Q_0) \rangle$$

$$\kappa_{\alpha}^{(i)} = \langle \Phi_i(Q_0) | \partial \mathbf{H}_{\text{el}} / \partial Q_{\alpha} | \Phi_i(Q_0) \rangle = \left. \frac{\partial V_i}{\partial Q_{\alpha}} \right|_{Q_0}$$

$$\lambda_{\alpha}^{(i,j)} = \langle \Phi_i(Q_0) | \partial \mathbf{H}_{\text{el}} / \partial Q_{\alpha} | \Phi_j(Q_0) \rangle = \left[\frac{1}{8} \frac{\partial^2}{\partial Q_{\alpha}^2} (|V_j - V_i|^2) \right] \Bigg|_{Q_0}^{1/2}$$

¹Jouybari, Liu, Improta, Santoro *J. Chem. Theory Comput.*, **2020**, *16*, 5792–5808

²Aleotti et al. *J. Chem. Phys.*, **2021**, *154*, 104106

$$\mathbf{H}^{\text{SO-vib}} = \mathbf{H}^{\text{SO}} + \mathbf{H}^{\text{vib}}$$

$$\mathbf{H}^{\text{vib}} = \mathbf{H}^{(0)} + \mathbf{W}^{(0)} + \mathbf{W}^{(1)} + \mathbf{W}^{(2)} + \dots$$

- The second order expansion term, $\mathbf{W}^{(2)}$, is the quadratic vibronic coupling (QVC) model
- These quadratic terms are responsible for changes in the frequency of the ground and excited state
- Must take into account Duschinsky rotation effects

- By using methods such as CASSCF and RASSI it will allow us to more accurately treat the electron correlation leading to more accurate results
- Will be able to build better PES than previously done with TD-DFT methods

- By using methods such as CASSCF and RASSI it will allow us to more accurately treat the electron correlation leading to more accurate results
- Will be able to build better PES than previously done with TD-DFT methods
- By exploring the similarities in the contributions from certain vibrational modes in the SVC we can run more efficient calculations which may decrease the computational cost

- By using methods such as CASSCF and RASSI it will allow us to more accurately treat the electron correlation leading to more accurate results
- Will be able to build better PES than previously done with TD-DFT methods
- By exploring the similarities in the contributions from certain vibrational modes in the SVC we can run more efficient calculations which may decrease the computational cost
- By studying the effect of O and C(CH₃)₂ on the intermediate triplet states we will be able to propose a molecule that may further enhance the k_{rISC} for more efficient emitters

Thank you!

$$k_{\text{rISC}} = \frac{2\pi}{3\hbar} \sum_M \sum_{\nu\nu'} P_\nu(T) |H'_M|^2 \delta(-\Delta_{\text{ST}} + E_\nu - E_{\nu'})$$
$$H'_M = H_{S_1T_1}^{\text{SO}} + \frac{1}{2} \sum_{T'} H_{S_1T'}^{\text{SO}} H_{T'T_1}^{\text{nBO}} \left(\frac{1}{E_{T'} - E_{T_1}} + \frac{1}{E_{T'} - E_{S_1}} \right)$$
$$+ \frac{1}{2} \sum_{S'} H_{S_1S'}^{\text{nBO}} H_{S'T_1}^{\text{SO}} \left(\frac{1}{E_{S'} - E_{T_1}} + \frac{1}{E_{S'} - E_{S_1}} \right)$$